Expansion of Polystyrene Using Supercritical Carbon Dioxide: Effects of Molecular Weight, Polydispersity, and Low Molecular Weight Components

Christopher M. Stafford, Thomas P. Russell,*,† and Thomas J. McCarthy*,‡

Polymer Science and Engineering Department, University of Massachusetts, Amherst, Massachusetts 01003

Received February 16, 1999; Revised Manuscript Received August 10, 1999

ABSTRACT: Closed cell foams of broad molecular weight distribution commercial polystyrene samples, prepared by expansion of supercritical-CO_2-swollen specimens, exhibit cell diameters that are ∼3−10 times (19−24 μm) larger than those of foams prepared from polystyrene samples with narrow molecular weight (NMW) distributions (∼2−6 μm). Cell diameters for NMW samples are independent of molecular weight from 147K to 1050K. Simulated polydisperse samples prepared by blending NMW distribution samples ranging from 560 to 1050K and a polydisperse sample prepared by radical polymerization produced foams with cells of the same size as in foams prepared from the NMW distribution samples. These observations suggest that molecular weight and polydispersity are not important factors in determining cell size and are not responsible for the disparity in cell sizes described above. This disparity is due to the presence of a very low molecular weight component (∼270) in the commercial samples. Extraction of this component reduced the cell diameter of resulting foams to that of the NMW distribution samples. Addition of a styrene oligomer (285) to a NMW distribution sample resulted in foams with larger cell diameters. Varying the concentration of this oligomer allows control of cell size in foams. Classical nucleation theory cannot explain these observations, suggesting that an alternative mechanism of cell formation is active.

Introduction

Supercritical (SC) fluids have received increased attention as alternatives to common solvents in areas such as polymerization,[1−3] polymer modification,[4−6] polymer fractionation,[7−9] and the preparation of microcellular foams.[10−13] Each of these areas utilize the unique properties of SC fluids, such as adjustable solvent strength (density), enhanced diffusivities, plasticization, and ease of removal to permit the design of innovative processes. Microcellular materials prepared by expansion of SC-fluid-swollen polymers are of interest due to the reduced amount of polymer needed to fabricate an article. Potential uses for these materials are in the areas of separation membranes, thermal and electrical insulation, and the generation of materials with enhanced mechanical properties.

One method for generating microcellular materials is by first saturating a polymer sample with an inert gas, such as N_2 or CO_2, and then rapidly immersing the sample in a high-temperature bath.[14,15] This temperature jump causes the polymer to soften by heating it above its glass transition temperature (T_g), thus allowing for the expansion of the absorbed gas. Quenching the sample brings the sample back below its T_g, vitrifying the polymer and locking in the resulting foamed structure. Recently Beckman et al.[10,11] reported a novel way of creating microcellular foams by use of SC CO_2. Using this method, a polymer sample is exposed to SC CO_2, which plasticizes the matrix and lowers the apparent T_g to near ambient temperatures. Upon rapid depressurization, the polymer matrix becomes supersaturated with CO_2 gas, nucleation of cells occurs and growth of these cells continues until the polymer vitrifies. The T_g rises as CO_2 leaves the matrix. The critical parameters controlling foam development in this process are the concentration of nuclei and the amount of time after depressurization before T_g rises to the temperature of the depressurization. These parameters dictate cell concentration, cell size, interstitial wall thickness, and the bulk density of the foam.

We recently reported[12,13] studies on polystyrene foams prepared using Beckman's technique. We found that temperature, initial pressure, depth of the pressure quench, decompression rate, decompression profile, and geometric constraints of the foaming vessel can be used to control cell size, cell size distribution, and cell shape as well as the compressive properties of the foams. Here we report the investigation of several other parameters that may affect the foaming process using SC CO_2 as the blowing agent. We address the effects of polymer molecular weight and polydispersity on the final structure of the foam using polystyrene and blends of polystyrene prepared by mixing samples with narrow molecular weight distributions. We also report the effect of a low molecular weight component found in commercial polystyrene samples and show that its presence dramatically changes the resulting foam structure. If the concentration of this oligomer is varied, control of the cell size in foams can be achieved.

Experimental Section

General Data. All materials were purchased from Aldrich and used as received, unless otherwise indicated. Anionic polymerization was carried out using standard Schlenk techniques. Styrene was stirred over CaH_2 for 24 h and distilled at reduced pressure. Just prior to polymerization, styrene was further dried by trap-to-trap distillation from Bu_2Mg, which forms a yellow solution indicating dryness. Benzene was dried by passing it through activated alumina to remove polar impurities and a copper catalyst (Q-5, Engelhardt) to remove

† E-mail: russell@mail.pse.umass.edu.
‡ E-mail: tmccarthy@polysci.umass.edu.

10.1021/ma9902100 CCC: $18.00
Published on Web 10/15/1999

traces of oxygen.[16] For radical polymerizations, styrene was distilled from CaH_2 and azobisisobutyronitrile (AIBN) was recrystallized from methanol. Glassware was dried at 135 °C for at least 12 h, assembled hot, flamed under vacuum, and then back-filled with nitrogen three times before addition of any reagents. Gastight syringes were dried at 135 °C for at least 12 h, flushed with nitrogen while cooling, and then fully assembled under constant nitrogen flow. Polymer molecular weights and distributions were determined by gel permeation chromatography (GPC) relative to calibration with polystyrene using a system equipped with Polymer Laboratories PL gel columns (10^4, 10^3, 10^2 Å), a Polymer Laboratories LC 1120 HPLC pump with THF as the mobile phase, and an IBM LC9563 Variable UV detector set at 254 nm. Differential scanning calorimetry (DSC) was performed using a DuPont Instruments DSC2910 and a heating rate of 10 °C/min. The polystyrene samples, PS^{514K} and PS^{1050K} and the MW 580 styrene oligomer were purchased from Polymer Laboratories; the MW 285 sample was obtained from Polysciences. Commercial polystyrene samples, $^{COM}PS^1$, $^{COM}PS^2$, and $^{COM}PS^3$ were purchased from SP^2, Acros, and Aldrich, respectively.

Polymerizations. To carry out anionic polymerizations, diluted (hexanes) *sec*-butyllithium was added via syringe to stirred benzene, followed by the addition of styrene via syringe. The polymerization was allowed to continue at room-temperature overnight and was then terminated with degassed methanol or ethanol. The polymer was precipitated into a 5-fold excess (based on the polymerization volume) of methanol, recovered by filtration, and dried under vacuum at 70−80 °C for several days. PS^{6K}, PS^{25K}, PS^{62K}, and PS^{147K} were prepared using this method.

Bulk radical polymerization of styrene was carried out in a 100 mL round-bottom flask to which AIBN (0.020 g) and styrene (50 mL) were introduced. This mixture was heated at 90 °C for 4 h, cooled, diluted with toluene, precipitated in methanol, recovered, and vacuum-dried as described above.

Sample Preparation. Blends of homopolymers were prepared by solvent casting from THF onto glass slides. The films were allowed to dry at room temperature for 1 day, dried under vacuum for 1 day, and finally dried at 120 °C for 6 h to remove last traces of solvent. The blends were then compression molded into $^1/_{32}$-in. plaques at 175 °C. Homopolymer samples were compression molded under the same conditions.

Foam Preparation. Foams were prepared in 316 stainless steel high-pressure vessels using an ISCO syringe pump to fill the vessels with SC CO_2. Samples were placed in high-pressure vessels, heated to 60 °C in a circulating bath, and filled to a pressure of 2050 psi (14.1 MPa) in convenient incremental stages. The vessels were then transferred to a circulating oil bath (100 °C) and maintained at this temperature for 3 h. At the end of this period, vessels were depressurized in ∼4 s at constant temperature. It should be noted that a slight cooling occurs inside the vessels due to the rapid expansion of the CO_2; thus, the actual depressurization temperature is less than 100 °C. The vessels were then removed from the temperature bath and allowed to cool to room temperature, and the samples were recovered.

Foam Characterization. The foams were characterized primarily by scanning electron microscopy (SEM). Samples were cryofractured after immersion in liquid N_2, sputter-coated with ∼200 Å of gold, and viewed using a JEOL 35CF SEM. The resulting micrographs were analyzed by Zeiss Image Analysis software to determine average cell diameters.

Results and Discussion

Sorption experiments[12] indicate that polystyrene can be swollen with supercritical carbon dioxide (SC CO_2) to a maximum level of ∼12 wt %. This swelling lowers the apparent glass transition to slightly above room temperature.[17] Upon decompression of the SC solution, the polystyrene foams as the sample becomes supersaturated with CO_2 gas. As the concentration of CO_2 in the polystyrene decreases (by partitioning into the pores), the glass transition temperature increases, and when it exceeds the temperature of the experiment, the sample vitrifies, freezing in the foam structure. The number and size of the pores in the foam depend on the concentration of CO_2 in the polystyrene, the number of nucleation sites, and the growth rate of the pores. The rate at which the CO_2 diffuses from the matrix to the growing pores depends on the temperature of the experiment, the pressure of the experiment and the viscosity of the swollen polymer. As a result of the viscosity dependence, the molecular weight and polydispersity of the polymer should influence the structure of the foam developed during decompression.

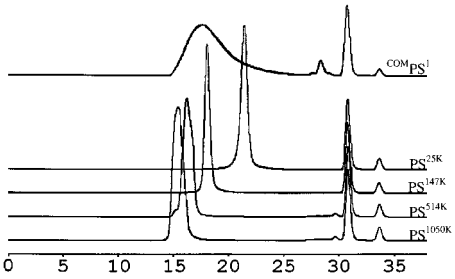

Figure 1. Gel permeation chromatograms of $^{COM}PS^1$, PS^{25K}, PS^{147K}, PS^{514K}, and PS^{1050K}.

Table 1. Polymer Sample Characteristics

sample	$10^{-3}M_n$	$10^{-3}M_w$	M_w/M_n	T_g, °C
PS^{6K}	6.6	6.8	1.03	95
PS^{25K}	24.4	25.4	1.04	104
PS^{62K}	62.1	64.0	1.03	107
PS^{147K}	147	153	1.03	108
PS^{514K}	514	540	1.05	107
PS^{1050K}	1030	1080	1.05	109
$^{COM}PS^1$	66.5	204	3.07	105
$^{COM}PS^2$	65.7	246	3.74	103
$^{COM}PS^3$	120	288	2.38	105
PS^R	96	214	2.22	106
$^BPS^1$	61	188	3.07	
$^BPS^2$	12.8	179	13.95	
$^BPS^3$	8.4	175	20.76	

Foaming experiments were performed on a series of narrow molecular weight distribution polystyrenes and commercial polystyrene samples of molecular weight and polydispersity summarized in Table 1. Size exclusion chromatograms for selected polymers are shown in Figure 1. Each of the narrow molecular weight distribution polymers shows a single sharp peak with differing retention times characteristic of the molecular weight of the polymer. The commercial polymer, $^{COM}PS^1$, shows a broad peak with a tail at long retention times indicative of lower molecular weight polymer. $^{COM}PS^1$ also exhibits a peak occurring at ∼28 min that corresponds to a molecular weight of ∼270.

Scanning electron micrographs of foams produced by decompression at 100 °C and 3400 psi (23.4 MPa) are shown in Figure 2. Cursory examination of these micrographs shows a striking difference between the commercial and narrow molecular weight distribution polystyrene samples. The cell size (diameter) in each of the narrow molecular weight distribution polymer foams is ∼5 μm. The results of image analysis of these micrographs are shown in Table 2. The cell size is independent of molecular weight over a very large molecular weight range. The only exception to this is the PS^{25K} sample, which shows a smaller cell diameter (2.2 μm). In marked contrast to this, the commercial foamed polymer exhibits a cell diameter of ∼24 μm; the

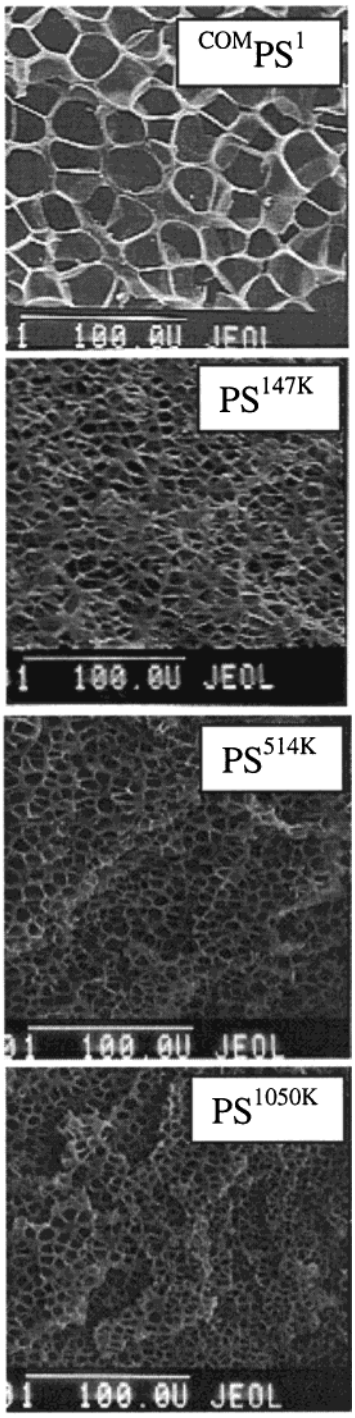

Figure 2. SEM micrographs of fracture surfaces of foams prepared from a commercial polystyrene sample and three narrow molecular weight distribution polystyrene samples.

cell diameter is nearly five times larger and the cell volume is greater than 100 times larger than those of the narrow molecular weight distribution polystyrenes.

Polystyrene samples from two other sources were examined to ensure that this behavior is not peculiar to one commercial polystyrene source. The characteristics of these polymers ($^{COM}PS^2$ and $^{COM}PS^3$) are given in Table 1. Size exclusion chromatograms for $^{COM}PS^2$ and $^{COM}PS^3$ are similar to that of $^{COM}PS^1$, and in particular, each contains a peak (of different intensity) that corresponds to a molecular weight of ~270. Figure 3 shows SEM micrographs of foams prepared using $^{COM}PS^2$ and $^{COM}PS^3$, indicating that the foams are very

Table 2. Average Cell Size Diameters of Foams

sample[a]	av cell diameter (μm)	cell density (no. of cells/cm^3)
PS^{25K}	2.2	4.11×10^{10}
PS^{147K}	5.3	4.28×10^{9}
PS^{514K}	5.9	2.16×10^{9}
PS^{1050K}	5.7	3.74×10^{9}
PS^{R}	4.7	2.36×10^{9}
$^{COM}PS^1$	24	6.54×10^{7}
$^{COM}PS^2$	24	1.21×10^{7}
$^{COM}PS^3$	19	1.83×10^{8}
$^{B}PS^1$	5.2	
$^{B}PS^2$	5.8	
$^{B}PS^3$	7.9	
$^{B}PS^4$	11.9	9.79×10^{8}
$^{B}PS^5$	13.9	5.18×10^{8}
$^{B}PS^6$	18.4	3.27×10^{8}
$^{COM}PS^{1EX1}$	8.9	1.12×10^{9}
$^{COM}PS^{1EX2}$	7.2	1.97×10^{9}
$^{COM}PS^{1EX3}$	5.9	3.24×10^{9}

[a] Superscripts with K indicate narrow molecular weight distribution samples, with COM indicate commercial broad molecular weight distribution samples, with B indicate a blend, and with EX indicate extracted samples.

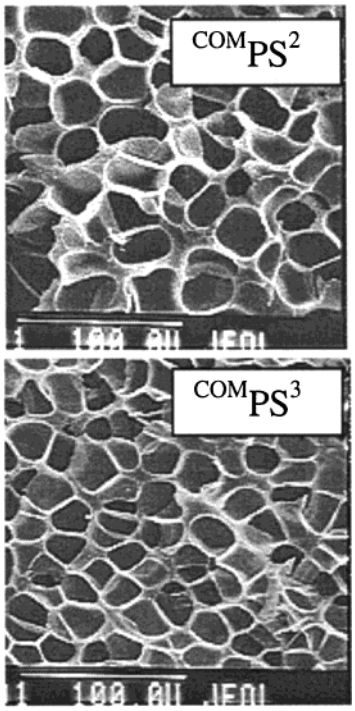

Figure 3. SEM micrographs of fracture surfaces of foams prepared from two different commercial polystyrene samples (compare with $^{COM}PS^1$ in Figure 2).

similar to foams prepared from $^{COM}PS^1$ (Figure 2), with large cell diameters of 19 and 24 μm, respectively.

The most obvious difference between the narrow molecular weight distribution polymers and the commercial materials is the molecular weight distribution. The large disparity between cell sizes indicates that either the nucleation density of the pores is much greater in the narrow molecular weight distribution polymer or that the growth rate of the pores is much faster for the broad molecular weight distribution polymer. This may arise from a change in the free energy associated with the formation of a nucleus of critical size or, in the case of homogeneous nucleation, a change in the growth rate of the pores. The increase in pore size for the broad molecular weight distribution polymer can also suggest that both high and low

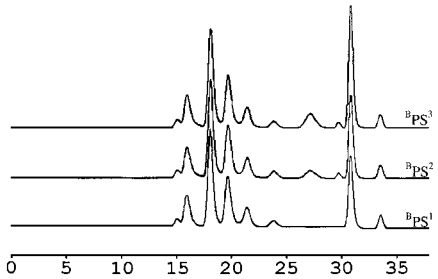

Figure 4. Gel permeation Chromatograms of simulated polydisperse polystyrene samples: $^{B}PS^{1}$, a 6-component blend of PS^{6K}, PS^{25K}, PS^{62K}, PS^{147K}, PS^{514K}, and PS^{1050K}, $^{B}PS^{2}$, a 7-component blend that contains the samples in $^{B}PS^{1}$ plus 7.4 wt % of a 560 styrene oligomer, and $^{B}PS^{3}$, which is the same as $^{B}PS^{2}$, except that it contains 13.0 wt % of the 560 oligomer.

molecular weight components are necessary to support the large cell structure. The high molecular weight component would serve to enhance the number of intermolecular entanglements, whereas the lower molecular weight component would promote rapid cell growth. To address this latter possibility, a polydisperse sample was prepared by blending several narrow molecular weight distribution polymers to yield a sample that had approximately the same M_n and M_w as $^{COM}PS^{1}$. This blend was comprised of six different molecular weight polystyrene samples, PS^{6K}, PS^{25K}, PS^{62K}, PS^{147K}, PS^{514K}, and PS^{1050K}. The simulated polydisperse sample had molecular weights of M_n = 61K and M_w = 188K (M_n/M_w = 3.07); the GPC chromatogram of this blend ($^{B}PS^{1}$) is shown in Figure 4. Foams from this sample, however, showed cell sizes in the range of 5−6 μm (Figure 5). The similarities in the cell size of the foams produced from the simulated polydisperse material and from the narrow molecular weight distribution polymers indicate that polydispersity is not critical in defining cell size. This was further demonstrated by foaming a polystyrene sample prepared by bulk free radical polymerization of styrene. GPC indicates that this sample (PS^{R}) has M_n = 96K and M_w = 214K (M_w/M_n = 2.22). The sample was foamed under identical conditions, and the cell sizes were ∼5 μm, identical to that of narrow molecular weight distribution polymers and the simulated polydisperse sample.

This result prompted a closer examination of any differences between the commercial materials and those prepared in our laboratories. The commercial samples show a peak in the size exclusion chromatogram at a retention time of ∼28 min which corresponds to a molecular weight of ∼270. This indicates the presence of a low molecular weight material, lower than any component of the simulated polydisperse sample. Consequently, a seventh component was added to the 6-component simulated polydisperse system ($^{B}PS^{1}$), a styrene oligomer of molecular weight of 580. Two blends were prepared with this oligomer, one with 7.4 wt % oligomer ($^{B}PS^{2}$) and one with 13 wt % oligomer ($^{B}PS^{3}$). The size exclusion chromatograms for these blends are shown in Figure 4, and the foam structures prepared with these samples are displayed in Figure 5. The average cell diameters were in the range of 6−8 μm, which is slightly greater than those of the narrow molecular weight distribution samples but much smaller than those of the commercial samples.

Using a different strategy to determine whether the low molecular weight component is responsible for the increase in cell size, this component was extracted from

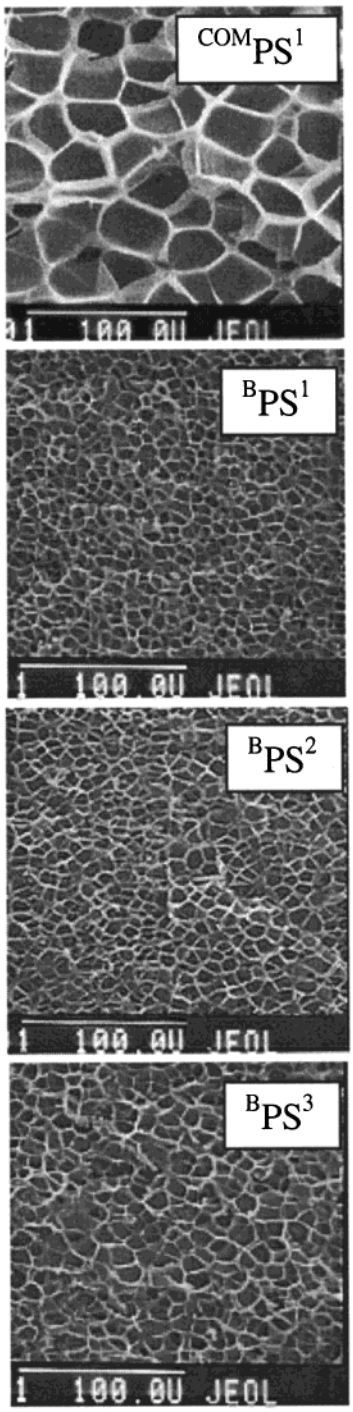

Figure 5. SEM micrographs of fracture surfaces of foams prepared from the simulated polydisperse polystyrene samples described in Figure 4 and $^{COM}PS^{1}$ (for comparison).

$^{COM}PS^{1}$ prior to foaming. $^{COM}PS^{1}$ was reprecipitated from a THF solution into methanol, filtered and vacuum-dried as described above. The first reprecipitation lowered the concentration of the oligomer from 3.8% to 1.3% as shown in Figure 6. The percentages reported here are area percentages obtained by dividing the area under the peak at 270 by the total area of the entire distribution, excluding the area due to the toluene flow marker (∼31 min) and beyond. The resulting foam ($^{COM}PS^{1EX1}$) shows pore sizes of 8.9 μm, as indicated in Figure 7. Second and third reprecipitations lowered the concentration of low molecular material to 0.9% and 0.1% respectively. The cell diameters in foams of these

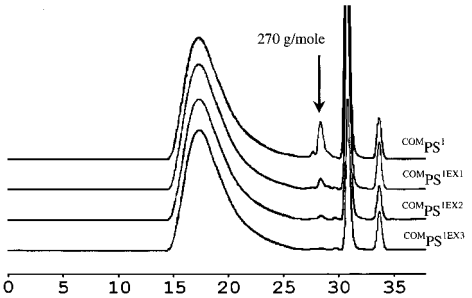

Figure 6. Gel permeation chromatograms showing the removal of a low molecular weight (LMW) component from ^{COM}PS^{1} by repeated reprecipitation from THF in methanol: ^{COM}PS^{1} (3.8% LMW component); ^{COM}PS^{1EX1} (1.3% LMW component); ^{COM}PS^{1EX2} (0.9% LMW component); ^{COM}PS^{1EX3} (0.1% LMW component).

samples (^{COM}PS^{1EX2} and ^{COM}PS^{1EX3}), as shown in Figure 7, are 7.2 and 5.9 μm, respectively, essentially identical, in the case of ^{COM}PS^{1EX3}, to those prepared with narrow molecular weight distribution samples. These results indicate that manipulating the concentration of this low molecular weight component can control cell size of the resulting foam.

To determine whether this low molecular weight component acts in a unique manner to affect foam structure, a polystyrene standard (styrene oligomer) having a molecular weight of 285 and a PDI of 1.20 was purchased. This low molecular weight sample was blended with PS^{147K}. Three different samples were made containing 3.6 wt % (^{B}PS^{4}), 7.3 wt % (^{B}PS^{5}), and 9.9 wt % (^{B}PS^{6}) of the MW 285 oligomer. The GPC chromatograms are shown in Figure 8. Foamed samples of pure PS^{147K} exhibit cell diameters ~5 μm (Table 2) before addition of any low molecular weight component. Upon addition of the MW 285 component, the resulting foams show an increase in cell size up to 19 μm for the 9.9 wt % sample, as shown in Figure 9. This indicates that there is nothing unique about the low molecular weight impurity found in the commercial samples, and that the effect of this low molecular weight component can be reproduced by the addition of a low molecular weight polystyrene standard. While the overall efficiency of the low molecular weight impurity in the commercial samples for cell diameter enhancement may be greater than that seen for the low molecular weight polystyrene (3.8 area % compared to 9.9 wt %), the end result in terms of pore density and size is the same. The presence of a low molecular weight component having a molecular weight of 270−285, but less than a molecular weight of 580 (which was added in the simulated polydisperse blends), leads to the formation of large cells having sizes in the range of 19−24 μm.

From the image analysis data, we can calculate the number of bubbles nucleated per cm^3 of the foam by applying a method proposed by Kumar and Suh.[18] The cell densities obtained for most of the samples discussed earlier are shown in Table 2. What is immediately obvious from these data is that the presence of this low molecular weight component (270) has a dramatic influence on cell density. Nearly a two-order of magnitude decrease in the cell density is evident. Since the glass transition temperature of the polymers and the extent of swelling of the polymers with SC CO_2 is the same, i.e., the depressed glass transition temperatures of the swollen polymers are essentially the same, we cannot attribute this difference to the rate of cell growth.

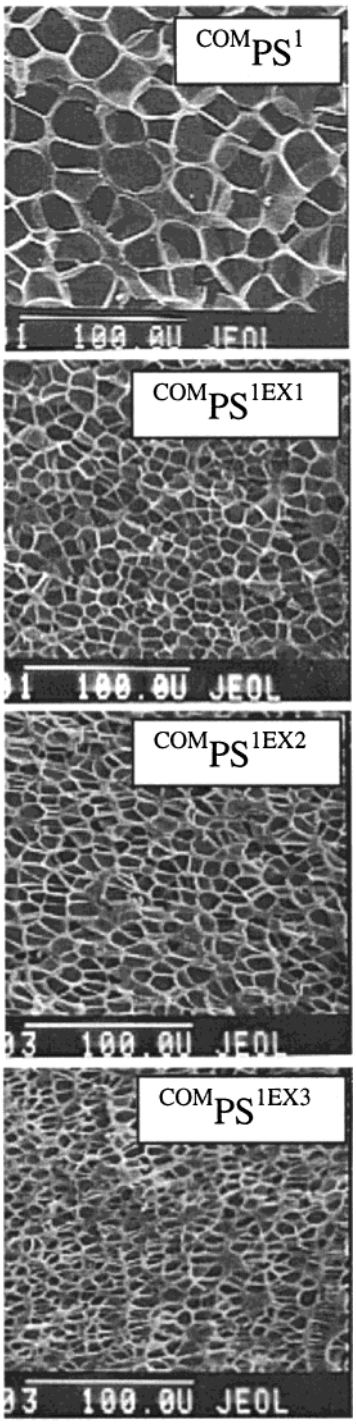

Figure 7. SEM micrographs of fracture surfaces of foams prepared from the samples described in Figure 6.

No evidence was found for cell coalescence. Consequently, the differences caused by the presence of the low molecular weight component must be attributed solely to a reduction in the number of nucleation sites.

Colton and Suh,[19−21] using classical nucleation arguments, derived an expression for the rate of nucleation of pores in microcellular foams. Whether the nucleation occurs by a homogeneous or heterogeneous process, the nucleation rate N is given by

$$N_i = f_i C_o \exp(-\Delta G_i^*/kT) \qquad (1)$$

where the subscript i denotes whether the nucleation is homogeneous or heterogeneous, f_i is a frequency factor

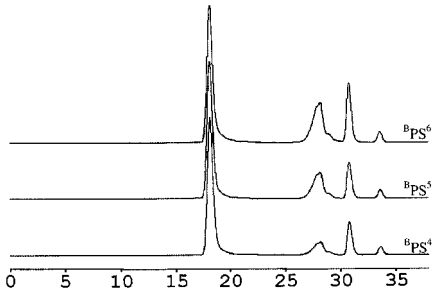

Figure 8. Gel permeation chromatograms of blends prepared from PS^{147K} and a 285 styrene oligomer: $^{B}PS^{4}$ (3.6 wt % oligomer), $^{B}PS^{5}$ (7.3 wt % oligomer), and $^{B}PS^{6}$ (9.9 wt % oligomer).

of gas molecules merging with the nucleus, C_o is the concentration of gas molecules, and ΔG_i^* is the Gibbs free energy associated with the formation of a nucleus. If the nucleation is homogeneous

$$\Delta G^* = \frac{16\pi\gamma^3}{3(\Delta P)^2} \tag{2}$$

where γ is the surface energy at the cell−polymer interface and ΔP is the pressure exerted by the SC CO_2 on the cell walls. In the case of heterogeneous nucleation

$$\Delta G^* = \frac{16\pi\gamma^3}{3(\Delta P)^2} f(\theta) \tag{3}$$

where the factor $f(\theta) = (^1/_4)(2 + \cos\theta)(1 - \cos\theta)^2$ and θ is the contact angle of the polymer/nucleation site/gas interface.

The dramatic changes in N observed in our studies cannot be explained by changes in either f_i or C_o. C_o is dictated by the swelling of the polymer by the SC CO_2, which is the same in all cases. While there may be changes in f_i due to the presence of the MW 270 component, a 2 order of magnitude change in f_i would not be expected based on the concentration of the impurity. Therefore, the change in nucleation density must originate with changes in ΔG^*, provided the mode of nucleation, i.e., homogeneous vs heterogeneous, remains unchanged. If N_i and N_i' are the cell nucleation rates in the absence of and presence of the low molecular weight component and the decrease in the nucleation rate is 2 orders of magnitude, then (assuming f_i and C_o are constant)

$$\ln\left(\frac{N_i'}{N_i}\right) = \ln(0.01) = -\frac{\Delta G^{*\prime} - \Delta G^*}{kT} \tag{4}$$

With a pressure drop of 3400 psi ($\sim 2.34 \times 10^8$ erg/cm^3), and using eqs 2 or 3, the change in the surface tension of the cells by the addition of the MW 270 component would be $\gamma' - \gamma = 9.2$ erg/cm^2. This result, however, shows that the presence of the low molecular weight component must increase the surface tension to bring about a reduction in the nucleation rate, a result that would contradict most results found in the literature.

Can the change in the nucleation rate be associated with a change in the mode of nucleation? Examination of all the cell structures produced in this study shows that the cell sizes are uniform; i.e., the distribution of cell sizes is narrow. A narrow cell size distribution requires that the nucleation sites be uniformly distributed in the system and that the nucleation of all the pores occurs within a narrow time regime. This is characteristic of a heterogeneous nucleation process with a uniform distribution of nucleation sites. Similar behavior is seen, for example, in the nucleation of polymer spherulites where, after crystallization, the spherulites have a characteristic size. Homogeneous nucleation, on the other hand, requires that nucleation occurs over a broad time period and would necessarily give rise to a broad distribution of cell sizes. No evidence was found in our studies to indicate that homogeneous nucleation occurred. Indeed, for most polymer systems, attaining conditions suitable for homogeneous nucle-

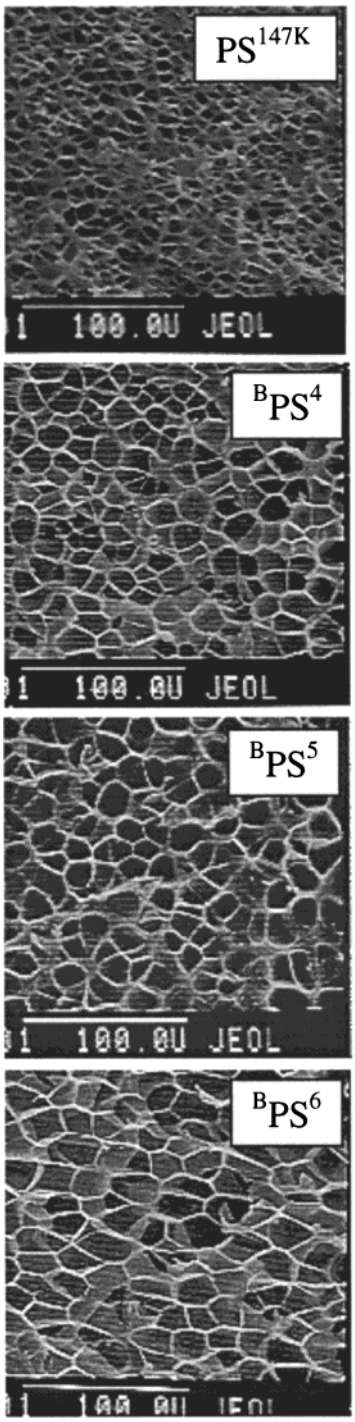

Figure 9. SEM micrographs of fracture surfaces of foams prepared from the simulated polydisperse polystyrene samples described in Figure 8 and PS^{147K} (for comparison).

ation is extremely difficult. Thus, contrary to the findings of Colton and Suh, where a dramatic reduction in the nucleation density was attributed to a change from homogeneous to heterogeneous nucleation, our data suggest that no such change has occurred.

Consequently, arguments based on nucleation and growth of cells fail to explain the observations described here. An alternative mechanism that needs to be considered is that of spinodal phase separation followed by a coarsening process. The system of SC-CO_2-swollen polymer is quenched into a metastable regime by a rapid pressure drop. Upon quenching, concentration fluctuations with many different length scales are present. With time, as a result of the balance between thermodynamics, which favors cell formation, and dynamics, which requires transport of the CO_2 molecules to the less dense regions, a characteristic wavelength begins to emerge. The amplitudes of the concentration fluctuations continue to grow until the saturation point, at which time a cell forms and begins to coarsen. The presence of the low molecular weight component could, in fact, serve to suppress the shorter wavelength fluctuations and lead to a reduction in the number of effective nucleation sites. Such a mechanism would lead to a uniform distribution of cells and, consequently, to a narrow distribution of cell sizes. A key element in this alternative mechanism of cell formation is the growth of concentration fluctuations with a characteristic wavelength. Studies are currently in progress using time-resolved X-ray scattering from quenched systems to investigate this. If the spinodal mechanism is active, a maximum in the scattering profile will be evident prior to cell formation, whereas with nucleation and growth, only a monotonic decrease in the scattering will be observed.

Conclusions

The effects of both molecular weight and sample polydispersity on SC CO_2 expansion of polystyrene has been examined in some detail. The data suggest that molecular weight and polydispersity do not significantly affect the foaming process. The presence of a low molecular weight component ($\sim$270), however, was found to greatly influence the final structure of the foam. This component does not have to be present in large amounts ($<$4%) to cause a substantial increase in cell size, and by adjusting its concentration, control of cell size can be achieved. Addition of a low molecular weight oligomer to polymer samples offers a way to control cell structure in SC CO_2 foaming systems. Small amounts of a low molecular weight polystyrene component produce nearly a 2 order of magnitude decrease in the nucleation density following the quenching of SC-CO_2-swollen PS. This reduced nucleation density gives rise to a 3−10-fold increase in the average cell diameter. Classical nucleation theory fails to explain the observations, suggesting that an alternative mechanism of cell formation, perhaps a spinodal mechanism, is active.

Acknowledgment. We thank the NSF-sponsored Materials Research Science and Engineering Center and the Office of Naval Research for financial support.

References and Notes

(1) Clark, M. R.; Kendall, J. L.; DeSimone, J. M. *Macromolecules* **1997**, *30*, 6011.
(2) Canelas, D. A.; Betts, D. E.; DeSimone, J. M.; Yates, M. Z.; Johnston, K. P. *Macromolecules* **1998**, *31*, 6794.
(3) Quadir, M. A.; DeSimone, J. M.; vanHerk, A. M.; German, A. L. *Macromolecules* **1998**, *31*, 6481.
(4) Watkins, J. J.; McCarthy, T. J. *Macromolecules* **1994**, *27*, 4845.
(5) Kung, E.; Lesser, A. J.; McCarthy, T. J. *Macromolecules* **1998**, *31*, 4160.
(6) Hayes, H. H.; McCarthy, T. J. *Macromolecules* **1998**, *31*, 4813.
(7) Pradhan, D.; Chen, C.; Radosz, M. *Ind. Eng. Chem. Res.* **1994**, *33*, 1984.
(8) Bungert, B.; Sadowski, G.; Arlt, W. *Fluid Phase Equilib.* **1997**, *139*, 349.
(9) Kumar, S. K.; Suter, U. W.; Reid, R. C. *Fluid Phase Equilib.* **1986**, *29*, 373.
(10) Goel, S. K.; Beckman, E. J. *Polym. Eng. Sci.* **1994**, *34*, 1137.
(11) Goel, S. K.; Beckman, E. J. *Polym. Eng. Sci.* **1994**, *34*, 1148.
(12) Arora, K. A.; Lesser, A. J.; McCarthy, T. J. *Macromolecules* **1998**, *31*, 4614.
(13) Arora, K. A.; Lesser, A. J.; McCarthy, T. J. *Polym. Eng. Sci.* **1998**, *38*, 2055.
(14) Colton, J. S.; Suh, N. P. *Polym. Eng. Sci.* **1987**, *27*, 485.
(15) Kumar, V.; Suh, N. P. *Polym. Eng. Sci.* **1990**, *30*, 1323.
(16) Pangborn, A. B.; Giardello, M. A.; Grubbs, R. H.; Rosen, R. K.; Timmers, F. J. *Organometallics* **1996**, *15*, 1518.
(17) Wang, W.-C. V.; Kramer, E. J.; Sachse, W. H. *J. Polym. Sci., Polym. Phys. Ed.* **1982**, *20*, 1371.
(18) Kumar, V.; Suh, N. P. *Polym. Eng. Sci.* **1990**, *30*, 1323.
(19) Colton, J. S.; Suh, N. P. *Polym. Eng. Sci.* **1987**, *27*, 485.
(20) Colton, J. S.; Suh, N. P. *Polym. Eng. Sci.* **1987**, *27*, 493.
(21) Colton, J. S.; Suh, N. P. *Polym. Eng. Sci.* **1987**, *27*, 500.

MA9902100